Fundamental Molecular Mechanism for the Cellular Uptake of Guanidinium-Rich Molecules

Henry D. Herce,[†,‡] Angel E. Garcia,*[,†] and M. Cristina Cardoso[‡]

[†]Department of Physics, Applied Physics and Astronomy and Center for Biotechnology and Interdisciplinary Studies, Rensselaer Polytechnic Institute, Troy, New York 12180, United States

[‡]Department of Biology, Technische Universität Darmstadt, 64287 Darmstadt, Germany

S *Supporting Information*

ABSTRACT: Guanidinium-rich molecules, such as cell-penetrating peptides, efficiently enter living cells in a non-endocytic energy-independent manner and transport a wide range of cargos, including drugs and biomarkers. The mechanism by which these highly cationic molecules efficiently cross the hydrophobic barrier imposed by the plasma membrane remains a fundamental open question. Here, a combination of computational results and in vitro and live-cell experimental evidence reveals an efficient energy-independent translocation mechanism for arginine-rich molecules. This mechanism unveils the essential role of guanidinium groups

and two universal cell components: fatty acids and the cell membrane pH gradient. Deprotonated fatty acids in contact with the cell exterior interact with guanidinium groups, leading to a transient membrane channel that facilitates the transport of arginine-rich peptides toward the cell interior. On the cytosolic side, the fatty acids become protonated, releasing the peptides and resealing the channel. This fundamental mechanism appears to be universal across cells from different species and kingdoms.
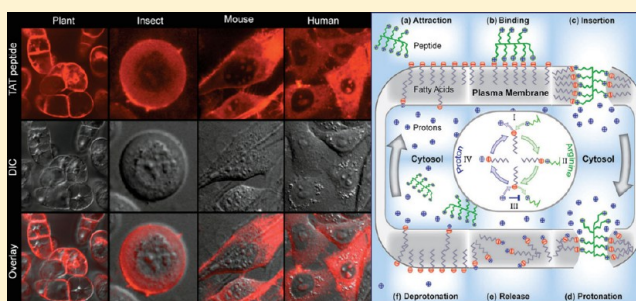
1. INTRODUCTION

Cell-penetrating peptides are short, usually arginine-rich amino acid sequences that are capable of transporting a wide range of biomolecules into virtually any living cell type.[1−8] There is abundant evidence that these peptides are able to directly translocate across the plasma membrane in an energy-independent and non-endocytotic manner, gaining free access to the cytosol and nucleus.[9−13] This challenges the fundamental concept that charged molecules cannot spontaneously diffuse across the cell membrane. The mechanism behind this puzzling effect follows three essential steps: (a) peptide binding to plasma membrane components; (b) spontaneous peptide absorption across the hydrophobic barrier imposed by the plasma membrane; and (c) breakage of the strong ionic binding between the peptide and the membrane when the peptide reaches the cytosol.

Arginine-rich peptides (RRPs) have strong affinities for multiple negatively charged plasma membrane groups. This affinity is so strong that removal of membrane-bound peptides requires enzymatic degradation of the peptides and the addition of strong counterions such as heparin to the wash solution.[14] However, it remains unclear whether any of these multiple cell membrane components could efficiently mediate the absorption of the RRPs into the hydrophobic core of the plasma membrane. It has been suggested that some membrane components could form stable complexes with RRPs, mediating their absorption into the core of the plasma membrane by forming either inverted micelles[15−17] or transient chan-

nels.[18−27] In both models, the peptides would reach the intracellular side of the cell membrane strongly bound to the cell membrane. Therefore, even if any of these mechanisms is right, there should be in place a common cellular mechanism to release these peptides from the cell membrane after they reach the cytosol.

Herein is described a complete cellular uptake mechanism for RRPs based on the ubiquitous interplay between two universal cell components: fatty acids and the plasma membrane pH gradient. We propose that at high pH fatty acids bind extracellular RRPs, mediate their membrane transport, and release them into the lower-pH environment of the cytosol. In vitro experiments presented here show all of the major steps of this mechanism. Computational results show that deprotonated fatty acids reduce the free energy of insertion of RRPs into model phospholipid bilayers and that this insertion leads to the formation of a channel across the lipid bilayer. Accordingly, live-cell experiments show that both the extracellular pH and the cell membrane fatty acid content modulate the cell transduction of RRPs into living cells. Furthermore, this mechanism describes the puzzling cell uptake differences observed between polyarginine and polylysine peptides. Finally, peptide uptake observations in multiple cell lines and the universality of the elements involved in this model (fatty acids
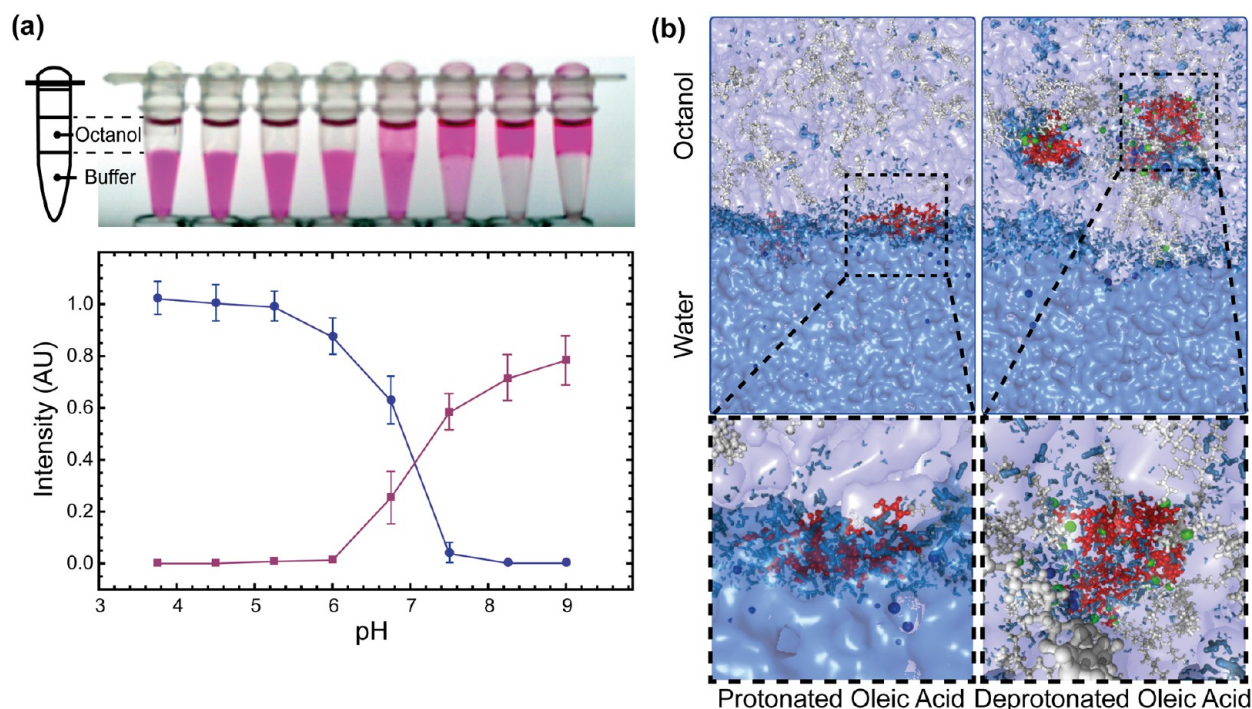
Figure 1. Within a physiological pH range, arginine-rich peptides can partition into an aqueous buffer at low pH and a hydrophobic environment at high pH. (a) Photograph showing that at pH less than 6.75 the TAT peptide (10 μM), labeled with TAMRA, partitions mainly into the aqueous phase, while at any pH higher than 6.75 the TAT peptide partitions mainly into the phase composed of octanol and 1% oleic acid. The plot shows the fluorescence emission of the peptide in each phase for each pH. While arginine and lysine amino acids do not change their protonation state within this range, fatty acids change from being neutral (protonated) at low pH to negatively charged (deprotonated) at high pH. (b) Snapshots after 300 ns molecular dynamics simulations of systems composed of 16 000 octanol molecules (represented with a white transparent surface), 64 protonated (left) or deprotonated (right) oleic acid molecules (the carbon chains of oleic acids are colored in white, while oxygens of protonated oleic acid are colored in gray and oxygens of deprotonated oleic acid are colored in green), four peptides (in red), 24 000 water molecules (blue surface; water molecules within 3 Å of any atom of the peptide or octanol or fatty acids are explicitly shown in blue), and chloride (left) or potassium (right) ions (in blue) to neutralize the system. When the fatty acids are protonated, the TAT peptides are excluded from the octanol phase, while when the fatty acids are deprotonated, the peptides partition in the octanol phase surrounded by fatty acids and water in a structure that resembles an inverted micelle.

and the cell pH gradient) suggest that this mechanism is universal across cells from different species and kingdoms.

2. RESULTS AND DISCUSSION

2.1. Protonation State of Fatty Acids Modulates RRP Binding. The central hypothesis of this work is that fatty acids can simultaneously mediate RRP membrane binding, membrane insertion, and cytosolic release. We postulate that this process is triggered by the pH gradient across the plasma membrane.

A simple in vitro model system to test this hypothesis is to study the distribution of RRPs between an aqueous buffer and octanol. Figure 1a shows a photograph displaying an aqueous buffer at different pHs in contact with an octanol phase containing 1% oleic acid. At pH less than 6.75, the TAT peptide (an RRP derived from the HIV-1 TAT protein) partitions mainly into the aqueous phase, while at any pH larger than 6.75, the TAT peptide is absorbed into the octanol phase. The plot shows the fluorescence emission intensity of the peptide labeled with TAMRA in each phase and at each pH value of the buffer. This indicates that fatty acids change from being neutral (protonated) at low pH to negatively charged (deprotonated) at high pH. Remarkably, the peptide absorption into the hydrophobic phase can be modulated within a physiological range very close to the extra- and intracellular pH in mammalian cells.

Figure S1 in the Supporting Information shows as a control this partition for the TAMRA dye alone, which partially partitions into the octanol phase at pH lower than 6, while for any higher pH the dye partitions only into the aqueous phase. This is the opposite behavior as when the dye is coupled to the TAT peptide (Figure 1a), indicating that the peptides drive the partition of the dyes into the aqueous phase at low pH and into the hydrophobic phase at high pH.

To obtain structural information on the peptides absorbed into the hydrophobic phase, we performed molecular dynamics simulations. Figure 1b shows a system composed of octanol, protonated (left) or deprotonated (right) oleic acid molecules, peptides, water, and chloride or potassium ions to balance the charges. We can see that when the fatty acids are protonated, the TAT peptides are excluded from the octanol phase, while when the fatty acids are deprotonated, the peptides partition into the octanol phase, forming a hydrophobic complex surrounded by fatty acids with a hydrophilic interior composed of water, ions, and the peptide. Therefore, peptides can be absorbed into octanol by forming structures with fatty acids that resemble inverted micelles with the polar groups in the interior of the structure.

We next explored whether other groups and hydrophobic environments would be able to modulate the absorption of arginine-rich peptides within a physiological pH range.

2.2. Fatty Acids Ubiquitously Modulate the Absorption of RRPs into a Hydrophobic Environment within a Physiological pH Range. In the absence of oleic acid, TAT does not enter the hydrophobic phase, as shown in Figure 2a. This indicates that the pH change only modulates the protonation of fatty acids. The pK_a of simple carboxyl acids is around 4.5, such as formic acid (pK_a = 3.77) or acetic acid (pK_a = 4.76), while the pK_a of fatty acids in pure monolayers is around 10. The pK_a, or apparent pK_a, of fatty acids depends on several factors such as the degree, type, and position of

Figure 2. Fatty acids ubiquitously modulate the partition of arginine-rich peptides within a physiological pH range. In the left column are shown snapshots of microcentrifuge tubes containing the different hydrophobic phases in contact with the aqueous buffers at different pHs. The right column shows the structures of the relevant components. The TAT peptide was labeled with TAMRA and excited with UV light (280 nm) to facilitate the visualization of the peptide distribution. (a) In the absence of carboxylic groups coupled to hydrophobic moieties, such as fatty acids, the TAT peptide does not partition into octanol. (b) In the presence of hydrophobic compounds containing phosphate and sulfur groups (100 μM in octanol) the TAT peptide (10 μM) partitions into the hydrophobic phase at every pH. These groups could help attract the peptides toward the plasma membrane. However, these groups fail to provide a mechanism for cytosolic release of membrane-bound peptides. On the other hand, other hydrophobic molecules containing carboxyl groups, such as lithocholic acid, display behavior similar to that of oleic acid, although in this case the deprotonation is shifted toward higher pH. (c) Partition of the TAT peptide into three distinct types of natural vegetable oils: sunflower oil, castor oil, and olive oil. Vegetable oils are rich in fatty acids. However, most of these fatty acids are not free but instead form triglycerides, which lack free carboxyl groups essential for the binding of RRPs.

unsaturation and the local environment,[28] and it has recently been shown that in cells this value could be shifted toward a physiological pH range.[29] On the other hand, the protonation state of guanidinium groups is very stable even in hydrophobic environments.[30]

It has been speculated that membrane phosphate and sulfur groups might be critical for the cellular uptake of RRPs, but it can be seen in Figure 2b that although these groups bind to RRPs, they remain bound at every pH. These groups could help attract the peptides toward the plasma membrane. However, they fail to provide a mechanism for cytosolic release of membrane-bound peptides. Furthermore, at the plasma membrane these groups are usually part of more complex molecules such as plasma membrane phospholipids that are more rigid and less likely to flip across the bilayer than simple fatty acids, thus providing stability to the plasma membrane. At high concentrations, these peptides can also penetrate and change the structure of phospholipid membranes,[27] and their toxicity at high concentrations might be a consequence of permanently destabilizing the phospholipid bilayer. All of these factors make less favorable the membrane absorption, translocation, and release of RRPs by complexation with plasma membrane components containing phosphate or sulfur groups. Figure 2b also shows that carboxyl groups present in other types of amphiphilic molecules, such as lithocholic acid, display behavior similar to that of oleic acid, although the deprotonation in this case is shifted to a higher pH, suggesting that other molecules containing a hydrophobic moiety coupled to carboxyl groups could analogously modulate the absorption of arginine-rich molecules. This could help explain recent works that have highlighted the specific role of pyrenebutyrate, originally suggested by Sakai and Matile,[15] as an enhancer of the cellular uptake of RRPs.[31,32] This particular enhancer is composed of a carboxyl group (from the butyric acid part of the molecule) followed by a hydrophobic structure (mainly from the aromatic pyrene part).

To explore these effects in richer hydrophobic environments, we also studied the partition of RRPs into three distinct types of natural vegetable oils: sunflower oil, castor oil, and olive oil. Vegetable oils are rich in fatty acids. However, most of these fatty acids are not free but instead form triglycerides, which lack free carboxyl groups essential for the binding of RRPs. We can see in Figure 2c that sunflower oil displays a behavior consistent with a composition of only triglycerides, displaying no absorption of the TAT peptide in the hydrophobic phase. Castor oil behaves as also having free fatty acids, showing an absorption behavior similar to that of oleic acid (Figure 1a). Olive oil displays absorption of the TAT peptide at the interface at every pH, revealing the presence of phospholipids.[33] This absorption remains constant until pH 6, followed by a clear increase in absorption at higher pHs produced by the additional presence of free fatty acids.

We next adapted the previous in vitro setup to test whether this mechanism would allow the spontaneous transfer of RRPs from a high- to a low-pH buffer across a hydrophobic barrier.

2.3. Fatty Acids Can Transport RRPs across a Hydrophobic Barrier. The proton gradient across the cell membrane can regulate fatty acid protonation and drive the cellular uptake of RRPs. Therefore, we asked whether this effect could be captured in an analogous in vitro assay. This assay should display the transport of cell-penetrating peptides from a high-pH buffer to a low-pH buffer across a hydrophobic barrier. Figure 3 shows that RRPs indeed diffuse across the octanol
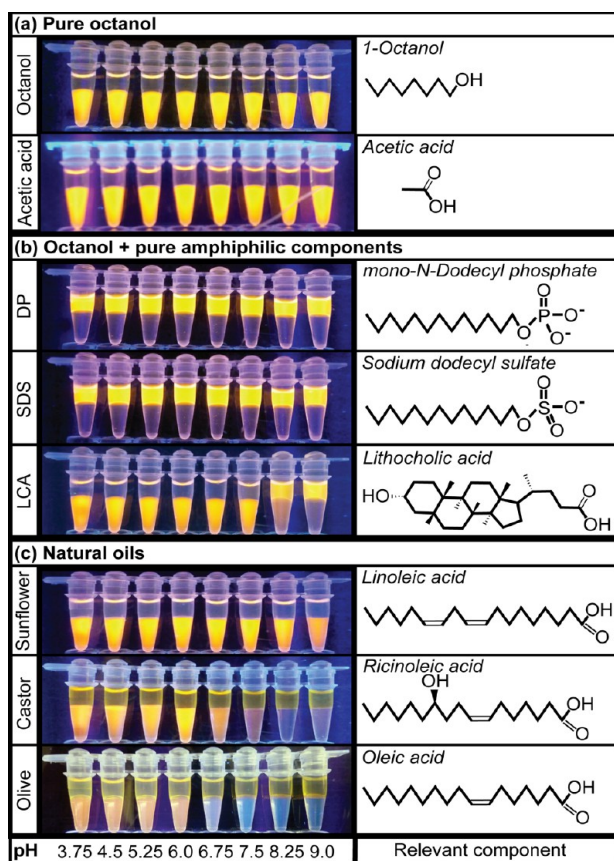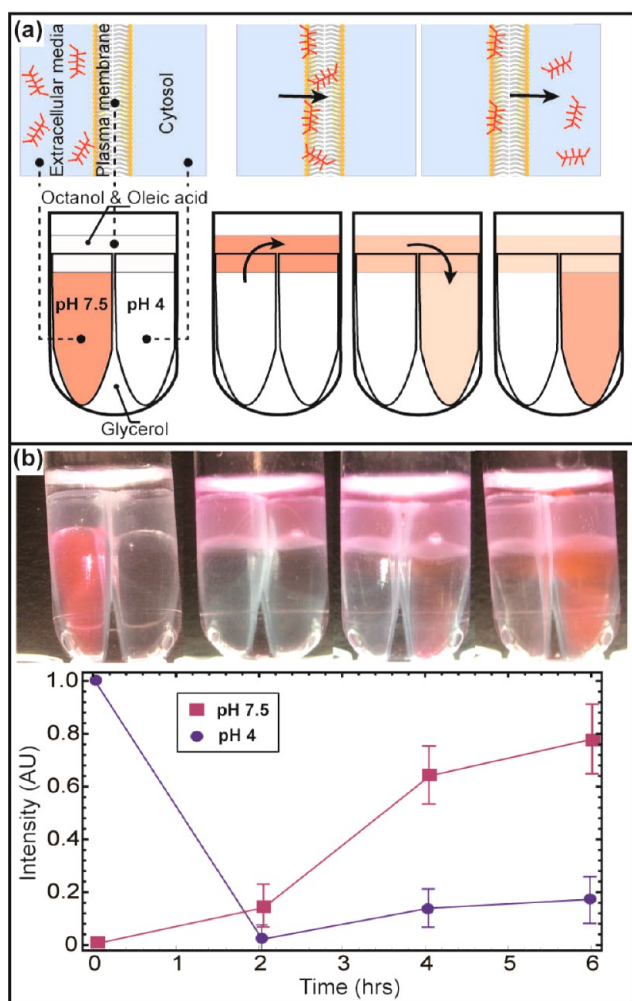
Figure 3. Arginine-rich cell-penetrating peptides can diffuse across a hydrophobic environment from a high- to a low-pH buffer in the presence of fatty acids. (a) Cartoon description of the cellular analogue of the in vitro setup, in which arginine-rich peptides are added to the extracellular medium at higher pH and diffuse across the membrane barrier toward the interior of cells at lower pH. The in vitro setup consists of two compartments at pH 7.5 and 4 connected by a layer of octanol and 1% oleic acid. The peptides were added to the high-pH compartment (pH 7.5), and they initially diffused into the hydrophobic phase and then at a lower rate into the low-pH buffer (pH 4). (b) Photographs of the setup and a plot of the peptide distribution (fluorescence emission) at different times. After 6 h, the peptides were mostly distributed between the octanol phase and the low-pH chamber.

hydrophobic barrier in the presence of fatty acids from a high-pH to a low-pH buffer. Figure 3a shows a cartoon illustration of the in vitro setup and its cellular analogue. The in vitro setup consists of two compartments at pH 7.5 and 4 connected by a layer of octanol with 1% oleic acid. Cells actively control the pH gradient across the plasma membrane, while in this experimental set up the pH is not actively maintained in each chamber. This could potentially lead to a fast pH equilibration between the two chambers as a consequence of the fatty-acid-mediated transfer of protons. Therefore, we chose a lower pH for the trans compartment than in the cytosol to ensure that the pH gradient between the two compartments would be maintained throughout the experiment. The TAT peptides were added to the pH 7.5 buffer. Figure 3b displays

photographs of the setup at 2 h intervals and a plot of the relative fluorescence intensity in each buffer at each time point. After 2 h the peptides get absorbed initially into the hydrophobic phase and then at a lower rate diffuse into the low-pH chamber. After 6 h, the peptides are mostly distributed between the octanol phase and the low-pH buffer. Therefore, fatty acids can mediate the transport of RRPs across a hydrophobic environment from a high- to a low-pH buffer, resembling the cellular uptake of RRPs. Furthermore, the low-pH buffer can be considered a trap for the peptides, as the peptides diffuse in one direction. The diffusion of the peptides across the hydrophobic environment is primarily determined not by the peptide concentration but instead by the proton concentration. This correlates with the observation that RRPs diffuse toward the interior of cells and that after the extracellular peptides are washed away the internalized peptides remain trapped in the cells.

We next asked how the protonation of fatty acids affects the absorption of RRPs in phospholipid bilayers.

2.4. Fatty Acids Lower the Plasma Membrane Energetic Barrier for RRPs. To understand how fatty acids affect the peptide–membrane interaction in more detail, we computed the free energy profiles for the insertion of a TAT peptide into model phospholipid bilayers composed of a mixture of 1,2-dioleoyl-*sn*-glycero-3-phosphocholine (DOPC) and oleic acid. Umbrella sampling was used to enhance the sampling along the free energy barrier imposed by the lipid bilayer. Essentially, an external harmonic potential was introduced, restraining the peptide at multiple positions across the bilayer. The contribution of this bias to the free energy was consistently removed using the WHAM method to obtain the free energy required to insert the peptide into the bilayer.[34−36] Figure 4 shows the structures and free energy profiles of three systems composed of a TAT peptide, water molecules, and a lipid bilayer made of DOPC and oleic acid molecules. Figure 4a presents snapshots of the atomic conformations of the three systems studied, with the peptide at the center of the bilayer. These structures show that in the presence of deprotonated fatty acids the peptide's charged residues are screened by deprotonated fatty acids that easily insert into the center bilayer. On the other hand, in the absence of deprotonated fatty acids the arginine and lysine residues cannot be easily screened at the center of the bilayer, leading the peptide to acquire an extended conformation to reach the phosphate groups of the more rigid phospholipids on the surface. Movies S1−S3 in the Supporting Information show structural changes as the TAT peptide is inserted into the bilayer and the relative free energy along this path for each case. These free energies are plotted in Figure 4b, where it can be seen that the addition of protonated fatty acids to the bilayer reduces by half the reported[36] free energy of insertion of the TAT peptide into pure DOPC bilayers. It can be seen that when all of the fatty acids are deprotonated, the free energy barrier is further reduced to 25 kJ/mol. This reduction is a consequence of efficient screening of the arginine and lysine residues by deprotonated fatty acids. This energetic barrier could be further reduced by the cell transmembrane potential,[16,37,38] which is not necessary for the transport across octanol.

It has been proposed that a possible mechanism of insertion of RRPs into the core of the bilayer might involve the formation of reverse micelles[39,40] with RRPs surrounded by ambiphilic counterions, resembling the structure shown in Figure 1b. However, we can see that in three independent
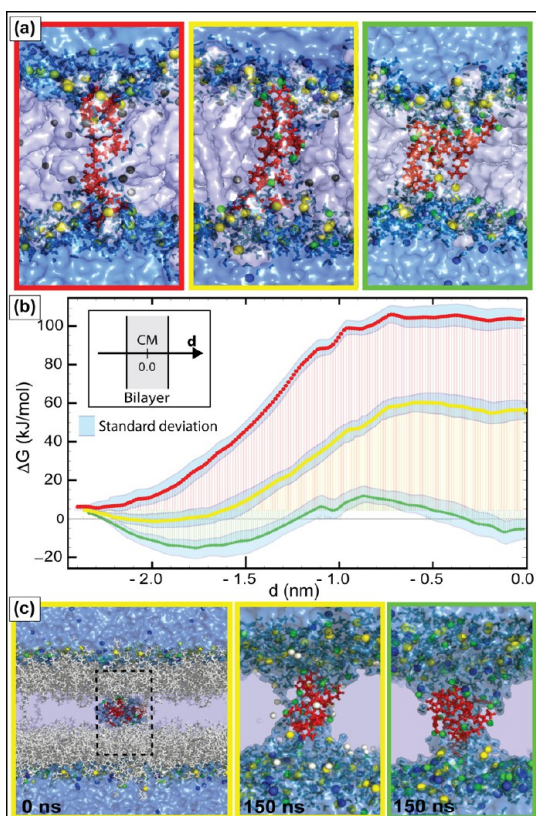
Figure 4. Structural analysis and free energy computations for insertion of the TAT peptide into phospholipid bilayers containing protonated and deprotonated fatty acids using molecular dynamics simulations. (a) Molecular conformations of the systems with the peptide constrained at the center of the bilayer. The systems are composed of a TAT peptide, 8700 water molecules, 68 DOPC molecules, and 48 oleic acid molecules (all protonated in red, half deprotonated in yellow, and all deprotonated in green). The systems are neutralized with the addition of potassium or chloride ions. Water is represented by a blue surface, with water molecules less than 3 Å from any atom of the peptide or lipid bilayer explicitly drawn in blue. DOPC and oleic acid molecules are shown with a white surface. Phosphate atoms are shown in yellow, protonated and deprotonated fatty acid carboxyl groups are shown in gray and green, respectively, and the TAT peptide is shown in red. (b) Free energy profiles as functions of the distance of the center of mass of the TAT peptide from the center of mass of the lipid bilayer. The total computed time for each free energy calculation profile was expanded to 10 μs. (c) To see whether an inverted-micelle-like structure would be stable at the center of the bilayer, we increased the bilayer size by a factor of 4 and inserted a single TAT peptide surrounded by water and oleic acid molecules that was previously equilibrated within a mixture of octanol and deprotonated fatty acids (Figure 1b). The final system was composed of 272 DOPC molecules, 200 oleic acid molecules, potassium counterions, 34 800 water molecules, and a TAT peptide. The peptide−fatty acid complex obtained from the simulation shown in Figure 1b was placed in the middle of the bilayer. The layers of the bilayer were separated, leaving significant space between the complex hydrophobic core and the surface of the bilayer, and from this conformation the systems relaxed to equilibrium for 150 ns at constant pressure. In the two cases tested, the initial structure resembling a reverse micelle transformed into a water-filled channel.

simulations (Figure 4a), when a peptide is inserted in the center of the bilayer, the lipid bilayer forms a water-channel structure.[18−20] To be sure that the system was not biased toward channel formation by the computed system size or the

initial structure, we performed a new computation in which the system was enlarged and the initial structure was biased toward the formation of an inverted-micelle-like structure in the center of the bilayer. In Figure 4c, we increased the bilayer size by a factor of 4 and inserted a single TAT peptide surrounded by water and deprotonated oleic acid using an initial structure from the simulations in Figure 1b resembling an inverted micelle. The peptide−fatty acid complex obtained from the simulation shown in Figure 1b was placed in the middle of the bilayer. The layers of the bilayer were separated, leaving significant space to fit the inverted-micelle-like structure, and from this conformation the systems relaxed at constant pressure to their final volume. In every case, the systems relaxed spontaneously to form a channel. This further supports that the insertion of RRPs into lipid bilayers leads to the formation of channels.[18−20]

Interestingly, it can also be observed that protonated fatty acids rapidly flip from one side of the bilayer to the other, while deprotonated fatty acids do not flip within this time scale. If the extracellular pH is much higher than the intracellular pH, any intracellular fatty acid that becomes protonated in the cytosol would rapidly flip, get deprotonated, and remain captured in the extracellular layer of the cell membrane. This implies that increasing the extracellular pH would greatly increase the number of deprotonated fatty acids in contact with the external side of the plasma membrane, leading to an enhancement of the cellular uptake of RRPs.

Cells actively control the intracellular pH, keeping it near neutral pH, but the extracellular pH can be chemically controlled. Therefore, we next asked whether altering the extracellular pH would modulate the uptake of RRPs into living cells consistently with the previous in vitro and molecular dynamics observations.

2.5. Extracellular Proton Density Modulates the Cellular Uptake of RRPs. Fatty acids are an integral part of all known cells. If this mechanism is also present in cells, then raising (lowering) the extracellular pH should enhance (reduce) the transduction of these peptides. Therefore, as shown in Figure 5 and movies S4−S9 in the Supporting Information, we compared the uptake of the TAT peptide when the extracellular pH was chemically controlled at different values. In most mammalian cells, the extracellular pH is close to 7.4. Therefore, we studied the peptide uptake in HeLa cells with the extracellular pH kept at 6, 7.5, and 9 using a HEPES buffer. Figure 5 shows time-lapse confocal microscopy snapshots of the uptake of the TAT peptide in living cells. While at this TAT peptide concentration (2 mM) there was no uptake at pH 6 and 7.5, most of the cells kept at pH 9 displayed significant uptake within this time interval (30 min). We also measured the change in the average fluorescence intensity of the entire image minus the background fluorescence (Figure 5), and we can see that at pH 6 and 7.5 this value remains negative, indicating that the concentration of membrane-bound and/or intracellular peptide is less than that in the extracellular medium, while at pH 9 the curve is positive, indicating clear cellular uptake.

This experiment was performed using an objective with 20× magnification, allowing the simultaneous visualization of several cells in the field of view. At this magnification it was difficult to resolve clearly whether the increase in fluorescence was correlated with cellular uptake and/or membrane-bound peptides. Therefore, to be able to differentiate intracellular from membrane-bound peptides within the same field of view,
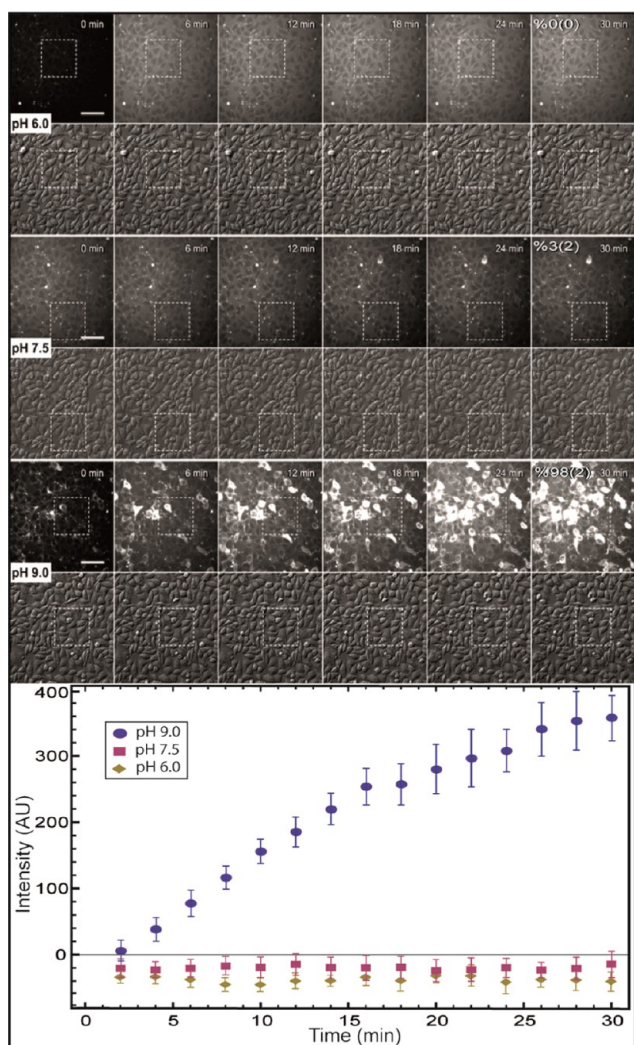
Figure 5. Increasing the extracellular pH consistently increases the transduction efficiency of arginine-rich peptides. Time-lapse fluorescence images show the TAT (2 μM) uptake in living cells at pH 6, 7.5, and 9. The lower plot shows the averages (over three independent repetitions) of the overall fluorescence intensity minus the background intensity and the standard errors of the mean as functions of time. After 30 min the fluorescence increased several-fold at pH 9 relative to pH 6 and 7.5. The images were acquired using an objective with 20× magnification. In this case, the membrane-bound peptide cannot be separated from the internalized peptide. To measure more strictly the free intracellular distributed peptide and compare it with these results, we simultaneously imaged the cells in the dotted regions using an objective with 60× magnification (Figure S2 in the Supporting Information). We measured the fluorescence intensity at the nucleolus relative to the background fluorescence over time and found that the two measurements gave analogous results. Scale bars = 75 μm.

we switched to a 60× objective (Figure S2 in the Supporting Information) to capture higher-magnification images of the dotted regions indicated in Figure 5. The plot in Figure S2 shows the fluorescence intensity in the nucleus minus the extracellular background fluorescence intensity. It can be seen that the internalized TAT peptide in the nucleus accumulated mainly at the nucleolus, from which it becomes easy to recognize that this fluorescence signal was produced only by free peptides and not by peptides trapped in endosomes or bound to the cell plasma membrane. Movies S4–S9 in the Supporting Information show the uptake of 2 μM TAT peptide

by HeLa cells at pH 6, 7.5, and 9 taken at 20× and 60× magnification. Cells were deprived of glucose and nutrients during peptide uptake, and no peptide trapped in endosomes was detected during this time. Cells tolerated these conditions, remaining viable. They preserved their morphology (as shown by differential interference contrast (DIC) images), remained enzymatically active (Figure S3 in the Supporting Information), and kept undergoing normal cell division (movie S10 in the Supporting Information).

We also tested the effect of the extracellular pH on the uptake of multiple RRPs with different lengths, structures, and chirality[8,41−43] using cell lines from different species and kingdoms (Figures S4−S9 in the Supporting Information). Increasing the extracellular pH resulted in an increase in cellular peptide uptake for all RRPs by all cell lines. Consistently in all of the cell lines studied here, at pH 6 there was almost no uptake of the peptide compared with pH 7.5 and 9. The fact that this behavior is common to cells from widely separated evolutionary organisms highlights the universality of the underlying mechanism that drives the cellular uptake of RRPs.

We asked next whether enriching the cells with fatty acids would also increase the uptake of RRPs.

2.6. Fatty Acid Plasma Membrane Enrichment Enhances Uptake of RRPs. Incubating cells in a medium enriched with fatty acids can increase the cell content of fatty acids.[44,45] Therefore, we first incubated the cells in a medium rich in fatty acids for 5 min and then washed and incubated the cells in a buffer at pH 7.5 with different concentrations of the TAT peptide (10, 5, and 2.5 μM). The cells were then washed and medium plus calcein was added to monitor for enzymatic activity, and the cells were imaged. In Figure 6 it can be seen that fatty-acid-enriched cells display a much higher uptake efficiency than the control cells and that most of the cells are viable as indicated by their morphology and enzymatic activity.

Polyarginine peptides (>7 amino acids long) efficiently transduce into living cells. However, this is not the case for polylysine peptides.[41,46] This is an intriguing result since both arginine and lysine residues remain positively charged over a broad physiological pH range. Therefore, fatty acids could analogously mediate the transport of polylysine peptides. We next asked whether fatty acids would consistently capture these remarkable differences.

2.7. Fatty Acids Capture Differences between Polyarginine and Polylysine. If fatty acids indeed play an active role in the cellular uptake of RRPs, then they should also consistently show a clear selectivity for arginine over lysine amino acids, making this a sensible test for the mechanism proposed here. Therefore, we first looked at the structure and energetics of the interaction between arginine amino acids (or guanidinium groups) and lysine amino acids (or amino groups) with the deprotonated carboxyl group of oleic acid. Using molecular dynamics simulations (Figure 7a), we computed the free energy as a function of the distance between the carboxyl carbon of oleic acid and the carbon (nitrogen) atom of the guanidinium (amino) group. This calculation shows that as the guanidinium group approaches the carboxyl group it encounters a free energy barrier of 1.8 kJ/mol, and the energy gained upon binding is 8.5 kJ/mol. In contrast, the amino group encounters a much higher free energy barrier of 6.1 kJ/mol, and the binding energy gain is only 2.5 kJ/mol. Therefore, guanidinium groups encounter an energetic barrier more than 3 times weaker to bind fatty acids relative to amino groups, and the relative gain in energy is more than 3 times higher.
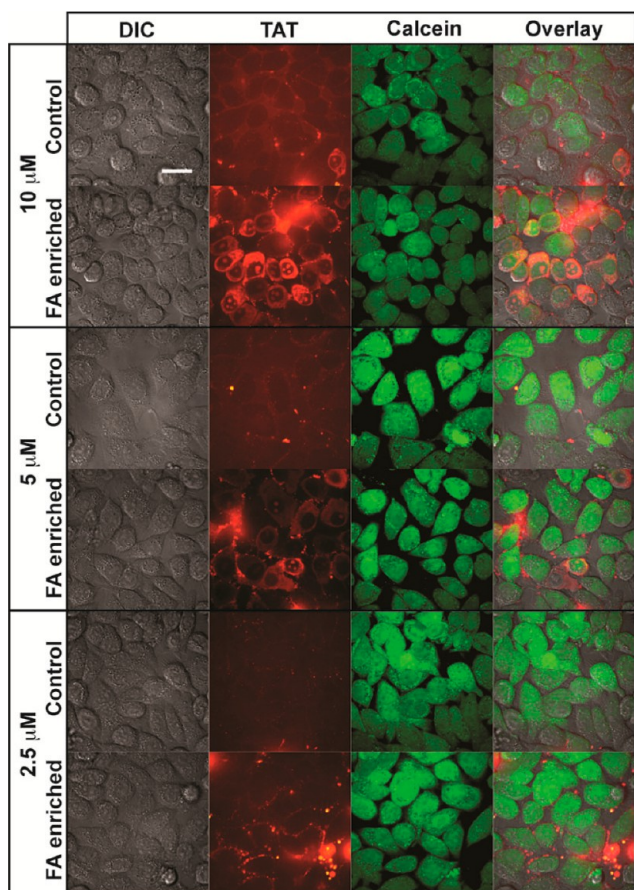
Figure 6. Enriching the plasma membrane with fatty acids enhances the binding and uptake of arginine-rich peptides. To test whether the cellular plasma membrane content of fatty acids can alter the uptake efficiency of RRPs, cells were incubated in a buffer rich in fatty acids for 15 min, washed, and incubated with added RRPs (10, 5, or 2.5 μM) for 5 min keeping the pH at 7.5. The cells were then washed and regular cell culture medium plus calcein was added, and the cells were imaged. In the first column are shown DIC images, in the second column the fluorescence emission of TAMRA-labeled TAT, in the third column the fluorescence intensity of calcein, and in the last column the overlay of the three channels. Scale bar = 25 μm.

Therefore, guanidinium groups bind more easily to fatty acids and in doing so gain significantly more energy. Figure 7b shows snapshots of the conformations of an arginine and a lysine amino acid at the position of the minimum free energy in each case.

Next, we experimentally tested the fatty acid absorption of polyarginine and polylysine peptides of different lengths in the octanol phase. Figure 7c shows experimental images of the partition of polyarginine and polylysine peptides between octanol with 1% oleic acid and aqueous phases at different pHs. We can see that K12 can be partially absorbed into the octanol phase at a higher pH than R12. R5 also partitions in the octanol phase at higher pH than R12, while K5 is unable to partition into the octanol phase within this pH range. Therefore, the interplay between fatty acids and proton density captures the essence of the puzzling observations reported in previous works showing that polylysines or short polyarginine sequences such as R5 are unable to efficiently transduce into living cells.
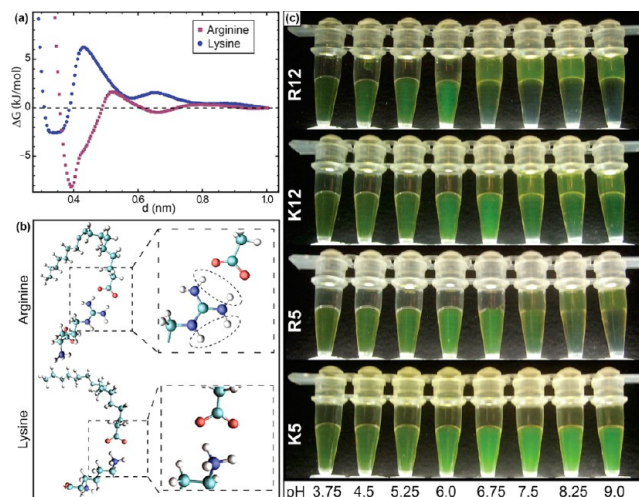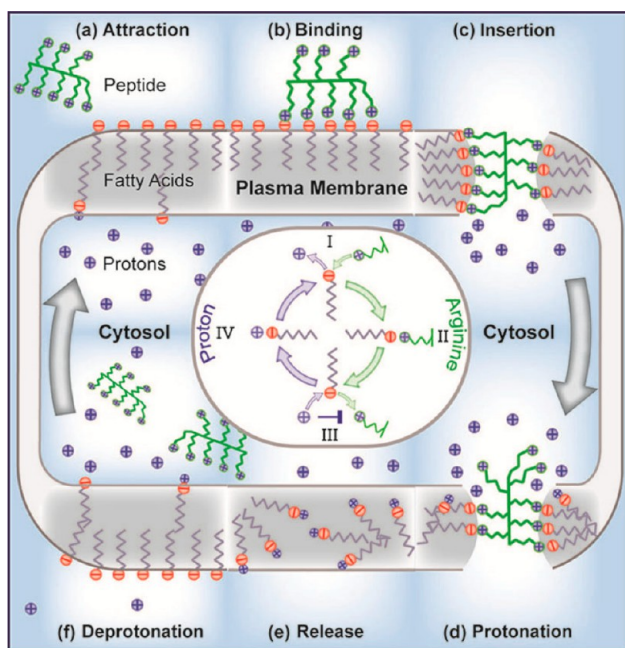

Figure 7. Arginine amino acids have a higher affinity for fatty acids than lysine amino acids. (a) Computed free energy profiles as functions of the distance between the carbon atom of the deprotonated carboxyl acid group (of the oleic acid) and the carbon atom of the guanidium group (arginine amino acid) or the carbon atom of the amino group (lysine amino acid). There is a gain in free energy 4 times higher for the binding of an arginine amino acid to an oleic acid relative to the binding of a lysine amino acid. (b) Snapshots of conformations of the amino acids at the positions where the free energy reaches a minimum, showing a more favorable alignment and hydrogen bonding in the case of the guanidinium group relative to the amino group. (c) Hydrophobic absorption of arginine and lysine amino acids at different pHs and numbers of residues. The photographs show polyarginine and polylysine peptides labeled with FITC in microcentrifuge tubes composed of two phases as described in Figure 1. The absorption into the hydrophobic phase is stronger for polyarginine peptides than for polylysine peptides. There is a sharp transition from the aqueous phase to the octanol phase at pH 6.75 for R12, while in the case of K12 this transition is shifted to a higher pH. Comparing R12 with R5, the absorption into the hydrophobic phase is shifted to a higher pH for R5, while K5 is not absorbed into the hydrophobic phase within this pH range.

3. CONCLUSION

Theoretical computations, in vitro and live-cell experiments reveal a mechanism in which fatty acids mediate the absorption and transport of RRPs across a hydrophobic barrier from a high- to a low-pH environment. This mechanism (depicted in Scheme 1) is essentially possible in cells because the intracellular pH in most cells is actively kept near neutral and at this pH plasma membrane fatty acids become protonated, while at a higher pH they become deprotonated. Deprotonated fatty acids in contact with the extracellular medium kept at higher pH bind to guanidinium groups with very high affinity, facilitating the absorption and peptide transport across the hydrophobic core of the plasma membrane nucleating a channel. In contact with the lower cytosolic pH, fatty acids become protonated and neutrally charged, and the RRPs are released from the plasma membrane into the cells and the channel closes. Protonated fatty acids freely diffuse across the plasma membrane, when in contact with the extracellular medium they get deprotonated, becoming negatively charged and trapped in the extracellular layer of the plasma membrane. Then, this cycle can then be repeated.

The possibility that these peptides might be able to directly cross the cell plasma has led, since their discovery, to a search for compounds that could enhance their cellular uptake. The

Scheme 1. Proposed Cellular Uptake Mechanism for Arginine-Rich Cell-Penetrating Peptides[a]

[a](a) The peptide located in the extracellular medium is attracted and (b) binds to deprotonated fatty acids. (c) The peptide–fatty acid complex nucleates a water channel. (d) This peptide–fatty acid complex diffuses across this channel while simultaneously protons from the cytosolic side compete for the binding of the guanidinium groups to fatty acids. (e) The high density of protons in the cytosol protonates the fatty acids, and the peptide gets released into the cytosol. (f) The channel closes, and neutral fatty acids freely diffuse across the plasma membrane; when they come into contact with the extracellular medium, they are deprotonated. The headgroups of the fatty acids become negatively charged and trapped in the extracellular layer of the plasma membrane, and the cycle can repeat again. The inset highlights that essentially fatty acids are able to get inserted into plasma membrane, transporting arginine-rich peptides (or guanidinium-rich molecules) toward the cytosol and protons toward the exterior of the cell. In the cytosol, fatty acids get protonated, inhibiting the binding of fatty acids to guanidinium groups.

mechanism outlined here explains at a fundamental level the enhancement effect of pyrenebutyrate on the cellular uptake of RRPs. The essential ingredients in the mechanism presented here are the guanidinium groups, the carboxyl groups coupled to a hydrophobic moiety, and the pH gradient across the plasma membrane. Accordingly, increasing any of these ingredients leads to a significant increase in transduction efficiency.

The mechanism uncovered by these experiments provides a unifying perspective on the cellular transduction of arginine-rich cell-penetrating peptides. The simplicity and universality of the elements involved in this mechanism elegantly reveals how these peptides are able to efficiently cross in an energy- and receptor-independent manner into virtually any cell type.

ASSOCIATED CONTENT

Ⓢ Supporting Information

Experimental and theoretical methods, chemical compounds, supporting figures, and supporting movies (AVI). This material is available free of charge via the Internet at http://pubs.acs.org.

AUTHOR INFORMATION

Corresponding Author

angel@rpi.edu

Notes

The authors declare no competing financial interest.

REFERENCES

(1) Frankel, A. D.; Pabo, C. O. *Cell* **1988**, *55*, 1189−1193.

(2) Bechara, C.; Sagan, S. *FEBS Lett.* **2013**, *587*, 1693−1702.

(3) MacEwan, S. R.; Chilkoti, A. *Wiley Interdiscip. Rev.: Nanomed. Nanobiotechnol.* **2013**, *5*, 31−48.

(4) Margus, H.; Padari, K.; Pooga, M. *Mol. Ther.* **2012**, *20*, 525−533.

(5) Walrant, A.; Bechara, C.; Alves, I. D.; Sagan, S. *Nanomedicine* **2012**, *7*, 133−143.

(6) Mussbach, F.; Franke, M.; Zoch, A.; Schaefer, B.; Reissmann, S. *J. Cell. Biochem.* **2011**, *112*, 3824−3833.

(7) Herce, H. D.; Deng, W.; Helma, J.; Leonhardt, H.; Cardoso, M. C. *Nat. Commun.* **2013**, *4*, No. 2660.

(8) Lättig-Tünnemann, G.; Prinz, M.; Hoffmann, D.; Behlke, J.; Palm-Apergi, C.; Morano, I.; Herce, H. D.; Cardoso, M. C. *Nat. Commun.* **2011**, *2*, No. 453.

(9) Tünnemann, G.; Cardoso, M. C. Cell-Penetrating Peptides— Uptake, Toxicity and Applications. In *Membrane-Active Peptides: Methods and Results on Structure and Function*; Castanho, M., Ed.; IUL Publishers: La Jolla, CA, 2009; pp 331−362.

(10) Ter-Avetisyan, G.; Tünnemann, G.; Nowak, D.; Nitschke, M.; Herrmann, A.; Drab, M.; Cardoso, M. C. *J. Biol. Chem.* **2009**, *284*, 3370−3378.

(11) Säälik, P.; Niinep, G.; Pae, J.; Hansen, M.; Lubenets, D.; Langel, Ü.; Pooga, M. *J. Controlled Release* **2011**, *153*, 117−125.

(12) Duchardt, F.; Fotin-Mieczek, M.; Schwarz, H.; Fischer, R.; Brock, R. *Traffic* **2007**, *8*, 848−866.

(13) Jiao, C.-Y.; Delaroche, D.; Burlina, F.; Alves, I. D.; Chassaing, G.; Sagan, S. *J. Biol. Chem.* **2009**, *284*, 33957−33965.

(14) Kaplan, I. M.; Wadia, J. S.; Dowdy, S. F. *J. Controlled Release* **2005**, *102*, 247−253.

(15) Sakai, N.; Matile, S. *J. Am. Chem. Soc.* **2003**, *125*, 14348−14356.

(16) Rothbard, J. B.; Jessop, T. C.; Lewis, R. S.; Murray, B. A.; Wender, P. A. *J. Am. Chem. Soc.* **2004**, *126*, 9506−9507.

(17) Esbjörner, E. K.; Lincoln, P.; Norden, B. *Biochim. Biophys. Acta* **2007**, *1768*, 1550−1558.

(18) Herce, H. D.; Garcia, A. E. *Proc. Natl. Acad. Sci. U.S.A.* **2007**, *104*, 20805−20810.

(19) Herce, H. D.; Garcia, A. E. *J. Biol. Phys.* **2007**, *33*, 345−356.

(20) Herce, H. D.; Garcia, A. E.; Litt, J.; Kane, R. S.; Martin, P.; Enrique, N.; Rebolledo, A.; Milesi, V. *Biophys. J.* **2009**, *97*, 1917−1925.

(21) Ciobanasu, C.; Siebrasse, J. P.; Kubitscheck, U. *Biophys. J.* **2010**, *99*, 153−162.

(22) Piantavigna, S.; McCubbin, G. A.; Boehnke, S.; Graham, B.; Spiccia, L.; Martin, L. L. *Biochim. Biophys. Acta* **2011**, *1808*, 1811−1817.

(23) Bouchet, A. M.; Lairion, F.; Ruysschaert, J.-M.; Lensink, M. F. *Chem. Phys. Lipids* **2012**, *165*, 89−96.

(24) Boll, A.; Jatho, A.; Czudnochowski, N.; Geyer, M.; Steinem, C. *Biochim. Biophys. Acta* **2011**, *1808*, 2685−2693.

(25) Choi, D.; Moon, J. H.; Kim, H.; Sung, B. J.; Kim, M. W.; Tae, J. Y.; Satija, S. K.; Akgun, B.; Yu, C.-J.; Lee, H. W.; Lee, D. R.;

Henderson, J. M.; Kwong, J. W.; Lam, K. L.; Lee, K. Y. C.; Shin, K. *Soft Matter* **2012**, *8*, 8294−8297.

(26) Chen, X.; Sa'adedin, F.; Deme, B.; Rao, P.; Bradshaw, J. *Biochim. Biophys. Acta* **2013**, *1828*, 1982−1988.

(27) Mishra, A.; Gordon, V. D.; Yang, L.; Coridan, R.; Wong, G. C. L. *Angew. Chem., Int. Ed.* **2008**, *47*, 2986−2989.

(28) Kanicky, J. R.; Shah, D. O. *J. Colloid Interface Sci.* **2002**, *256*, 201−207.

(29) Salentinig, S.; Sagalowicz, L.; Glatter, O. *Langmuir* **2010**, *26*, 11670−11679.

(30) Harms, M. J.; Schlessman, J. L.; Sue, G. R.; Garcia-Moreno E., B. *Proc. Natl. Acad. Sci. U.S.A.* **2011**, *108*, 18954−18959.

(31) Katayama, S.; Nakase, I.; Yano, Y.; Murayama, T.; Nakata, Y.; Matsuzaki, K.; Futaki, S. *Biochim. Biophys. Acta* **2013**, *1828*, 2134−2142.

(32) Guterstam, P.; Madani, F.; Hirose, H.; Takeuchi, T.; Futaki, S.; EL Andaloussi, S.; Gräslund, A.; Langel, Ü. *Biochim. Biophys. Acta* **2009**, *1788*, 2509−2517.

(33) Hatzakis, E.; Koidis, A.; Boskou, D.; Dais, P. *J. Agric. Food Chem.* **2008**, *56*, 6232−6240.

(34) Torrie, G. M.; Valleau, J. P. *J. Comput. Phys.* **1977**, *23*, 187−199.

(35) Herce, D. H.; Perera, L.; Darden, T. A.; Sagui, C. *J. Chem. Phys.* **2005**, *122*, No. 024513.

(36) Huang, K.; Garcia, A. E. *Biophys. J.* **2013**, *104*, 412−420.

(37) Henriques, S. T.; Costa, H.; Castanho, M. A. R. B. *Biochemistry* **2005**, *44*, 10189−10198.

(38) Tünnemann, G.; Martin, R. M.; Haupt, S.; Patsch, C.; Edenhofer, F.; Cardoso, M. C. *FASEB J.* **2006**, *20*, 1775−1784.

(39) Stanzl, E. G.; Trantow, B. M.; Vargas, J. R.; Wender, P. A. *Acc. Chem. Res.* **2013**, *46*, 2944−2954.

(40) Derossi, D.; Calvet, S.; Trembleau, A.; Brunissen, A.; Chassaing, G.; Prochiantz, A. *J. Biol. Chem.* **1996**, *271*, 18188−18193.

(41) Tünnemann, G.; Ter-Avetisyan, G.; Martin, R. M.; Stöckl, M.; Hermann, A.; Cardoso, M. C. *J. Pept Sci.* **2008**, *14*, 469−476.

(42) Herce, H. D.; Rajan, M.; Lättig-Tünnemann, G.; Fillies, M.; Cardoso, M. C. *Nucleus* **2014**, DOI: 10.4161/nucl.36290.

(43) Futaki, S.; Suzuki, T.; Ohashi, W.; Yagami, T.; Tanaka, S.; Ueda, K.; Sugiura, Y. *J. Biol. Chem.* **2001**, *276*, 5836−5840.

(44) Martin, P.; Moncada, M.; Enrique, N.; Asuaje, A.; Capuccino, J. M. V.; Gonzalez, C.; Milesi, V. *Pflügers Arch.* **2014**, *466*, 1779−1792.

(45) Schroit, A. J.; Gallily, R. *Immunology* **1979**, *36*, 199−205.

(46) Wender, P. A.; Mitchell, D. J.; Pattabiraman, K.; Pelkey, E. T.; Steinman, L.; Rothbard, J. B. *Proc. Natl. Acad. Sci. U.S.A.* **2000**, *97*, 13003−13008.

■ NOTE ADDED AFTER ASAP PUBLICATION

Figure 2 was corrected on December 2, 2014.